

Finite Difference anisotropic formulations for the EEG forward problem

P. Bruno,
DEEI & BRAIN,
University of
Trieste, Italy
bruno@deei.units.it

J. Hyttinen,
Ragnar Granit Institute,
Tampere University of
Technology, Finland
jari.hyttinen@tut.fi

P. Inchingolo, A. Magrofuoco, F. Meneghini,
S. Mininel and F. Vatta
DEEI & BRAIN, University of Trieste, Italy
paolo.inchingolo, magrofuoco, meneghini,
mininel, vattafe@deei.units.it

Abstract

In this paper we describe a new finite-difference method (FDM) EEG forward problem formulation which accounts for anisotropy of the various head tissues in the volume conductor model of the head. Our proposal, being based on FDM, derives the head model directly from patient's specific clinical images. We present here the numerical FD formulation and the comparison of the proposed method with a previously developed FD formulation with respect to known analytical results, using a multi-shell anisotropic head model with skull anisotropy. Furthermore, we analyzed also different numerical grid refinement and EEG source characteristics. The comparative analysis performed shows the validity of the proposed method.

1. Introduction

The computation of the electric potential generated by current density sources in the brain is the so-called EEG forward problem [1]. To get an accurate solution it is necessary to correctly model the shape of the head and tissues electrical conductivity [1], even in the presence of the anisotropy which characterizes tissues as white matter or the skull and is described by a conductivity tensor. Information about tissue anisotropy can be extracted from the Diffusion Tensor (DT-MRI) images and passed to the EEG forward problem formulation. Finite Difference (FD) models allow an image-based incorporation of such tissue complexities [2]. A FD formulation able to account for conductivity anisotropy as straightforward as possible from imaging information is therefore desirable. We propose an original FD problem formulation, valid for generally inhomogeneous and anisotropic structures, which is conceived to meet these needs [2]. While the Saleheen and Kwong's formulation [3] differs from standard FD formulations, since voxels are mapped as

mesh elements and mesh nodes correspond to voxels' vertexes, the formulation we propose considers the voxels' centre as the mesh's nodes and the computational points set in the voxels' center with a one-to-one correspondence between nodes and voxels, avoiding preliminary pre-processing due to the specific geometry of the adopted mesh. To test the validity of this new approach, simulation results of the proposed formulation are compared with an analytical forward problem solution for a 4-shell spherical head model with anisotropic skull [4], in comparison with the FD Saleheen and Kwong's formulation [3].

2. The FD formulation

Problem formulation starts from Poisson's equation $\nabla \cdot (\bar{\sigma} \nabla u) = \nabla \cdot \mathbf{J}$, with u the electric potential, $\bar{\sigma}$ the 3-D conductivity tensor and \mathbf{J} the current density. After expanding ∇ in the corresponding derivatives along x , y and z directions, the Taylor series expansions around a central node (node 0 in Fig. 1) up to the 2nd order can then be developed for the products of the conductivities and potentials (σu) at the neighboring nodes (1-18), generating a system of 18 equations. Solving these equations, the 1st and 2nd order partial derivatives of u at node 0 along x , y , and z can be expressed in terms of u and σ at all the nodes (0-18). The expression of u at node 0 in terms of u and σ at the surrounding nodes (1-18) is then finally obtained, containing the derivative of σ associated with the node corresponding to that voxel. Considering the conductivity to be constant over a voxel and formulating the conductivity of the general term $\sigma_{i,j(k)}$ taken as the average of the term $\sigma_{i,j}$ at node k and node 0, with $i=x,y,z$, $j=x,y,z$ and $k=1, \dots, 18$, a sort of smooth conductivity transition between the mesh elements can be achieved, guaranteeing also accurate results and increasing the speed of convergence. The final FD formulation is reported in eq. 1 as:

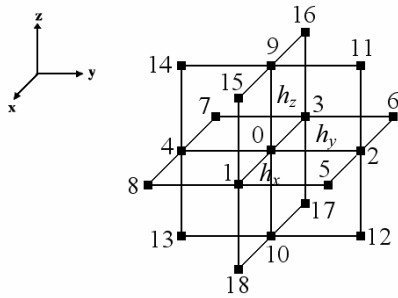


Figure 1. Indexes used in formulas for central node of the FDM computation and the surrounding neighboring nodes.

$$\sum_{i=1}^{18} A_i u_i = \left(\sum_{i=1}^{18} A_i \right) u_0 \quad (1)$$

with

$$\begin{aligned} A_1 &= \frac{1}{2h_x^2} (\sigma_{xx}^{[1]} + \sigma_{xx}^{[0]}), \quad A_2 = \frac{1}{2h_y^2} (\sigma_{yy}^{[2]} + \sigma_{yy}^{[0]}), \quad A_3 = \frac{1}{2h_x^2} (\sigma_{xx}^{[3]} + \sigma_{xx}^{[0]}), \\ A_4 &= \frac{1}{2h_y^2} (\sigma_{yy}^{[4]} + \sigma_{yy}^{[0]}), \quad A_5 = \frac{\sigma_{xy}^{[5]} + \sigma_{xy}^{[0]}}{4h_x h_y}, \quad A_6 = -\frac{\sigma_{xy}^{[6]} + \sigma_{xy}^{[0]}}{4h_x h_y}, \\ A_7 &= -\frac{\sigma_{xy}^{[7]} + \sigma_{xy}^{[0]}}{4h_x h_y}, \quad A_8 = -\frac{\sigma_{xy}^{[8]} + \sigma_{xy}^{[0]}}{4h_x h_y}, \quad A_9 = \frac{1}{2h_z^2} (\sigma_{zz}^{[9]} + \sigma_{zz}^{[0]}), \\ A_{10} &= \frac{1}{2h_z^2} (\sigma_{zz}^{[10]} + \sigma_{zz}^{[0]}), \quad A_{11} = \frac{\sigma_{yz}^{[11]} + \sigma_{yz}^{[0]}}{4h_y h_z}, \quad A_{12} = -\frac{\sigma_{yz}^{[12]} + \sigma_{yz}^{[0]}}{4h_y h_z}, \\ A_{13} &= \frac{\sigma_{yz}^{[13]} + \sigma_{yz}^{[0]}}{4h_y h_z}, \quad A_{14} = -\frac{\sigma_{yz}^{[14]} + \sigma_{yz}^{[0]}}{4h_y h_z}, \quad A_{15} = \frac{\sigma_{xz}^{[15]} + \sigma_{xz}^{[0]}}{4h_x h_z}, \\ A_{16} &= -\frac{\sigma_{xz}^{[16]} + \sigma_{xz}^{[0]}}{4h_x h_z}, \quad A_{17} = \frac{\sigma_{xz}^{[17]} + \sigma_{xz}^{[0]}}{4h_x h_z}, \quad A_{18} = -\frac{\sigma_{xz}^{[18]} + \sigma_{xz}^{[0]}}{4h_x h_z}. \end{aligned}$$

Indexes [.] refer to the voxel to which tensor entry refers. This formulation presents a leading error of h^2 with a linear system matrix symmetric, semi-definite positive and sparse (19 non-zero sub-diagonals).

3. Simulations and results

Results of forward problem computations performed by means of Saleheen and Kwong's formulation [3] (Method 1, named M1) and with the proposed FD formulation (Method 2, M2) are presented in Table 1. Simulations were performed with a 4-shell anisotropic concentric-spheres head model, composed by scalp, skull, cerebrospinal fluid and brain compartments with radii of 9.2, 8.7, 8.2 and 8 cm respectively. Adopted conductivities were: 0.33 S/m for scalp and brain, 1.0 S/m for CSF, 0.0047 and 0.0474 S/m for radial and tangential skull conductivities. Four dipole sources have been simulated, placed at 1.5, 3, 4.5 and 6 cm of distance from model center, radially or tangentially oriented. Potentials computed on the outer model's surface by

Methods 1 and 2 have been compared with the analytical solution [4] in the same test condition by means of the correlation coefficient (CC), defined as:

$$CC = \sqrt{\frac{\sum_{i=1}^N (u_i - \bar{u})(\hat{u}_i - \bar{\hat{u}})}{\left(\sum_{i=1}^N (u_i - \bar{u})^2 \right) \left(\sum_{i=1}^N (\hat{u}_i - \bar{\hat{u}})^2 \right)}} \quad (2)$$

where u_i and \hat{u}_i are the potentials at node i , in the analytical and in the FDM solution respectively, while \bar{u} and $\bar{\hat{u}}$ represent the mean values. CC close to 1 means a good fit of analytical and numerical solutions. Three different meshes have been tested, with 40^3 , 80^3 , and 100^3 nodes and inter-node distances of 5, 2.5 and 2 mm respectively.

Table 1. CC values for comparison between Method 1 (M1) and Method 2 (M2) for the three different meshes (test sources: P: position [cm]; O: orientation; R: radial; T: tangential).

Source	O	Mesh size					
		40^3		80^3		100^3	
		M1	M2	M1	M2	M1	M2
1.5	R	0.993	0.991	0.998	0.997	0.999	0.999
3.0	R	0.971	0.965	0.994	0.988	0.997	0.993
4.5	R	0.929	0.903	0.987	0.970	0.993	0.984
6.0	R	0.855	0.781	0.976	0.941	0.987	0.968
1.5	T	0.995	0.995	0.997	0.997	0.998	0.999
3.0	T	0.980	0.980	0.991	0.990	0.994	0.993
4.5	T	0.949	0.944	0.982	0.973	0.989	0.985
6.0	T	0.887	0.868	0.972	0.945	0.983	0.968

Errors in scale, measured using the MAG index [3], show similar results with M1 and M2. CC shows, in all the situations, a value close to 1 confirming the validity of M2 in comparison with M1. Even if M1 generally provides values of CC slightly higher, M2 implies, for the same model, building a smaller model mesh (N^3 elements instead of $(N+1)^3$) and hence a smaller linear system to be solved. This gain may be small if system is large, but the discretization approach of M2 allows a simpler implementation of the algorithm as it provides a one-to-one correspondence between voxels and mesh nodes.

References

- [1] F. Vatta, P. Bruno, P. Inchingolo, "Multiregion bicentric-spheres models of the head for the simulation of bioelectric phenomena," *IEEE Trans. Biomed. Eng.*, 52:384-389, 2005.
- [2] P. Bruno, J. Hyttinen, P. Inchingolo, A. Magrofuoco, S. Mininel, F. Vatta, "A FDM anisotropic formulation for EEG simulation," *Proc. 28th IEEE-EMBSConf.*:1121-1125, 2006.
- [3] H.I. Saleheen, T.N. Kwong, "New FD formulations for general inhomogeneous anisotropic bioelectric problems," *IEEE Trans. Biomed. Eng.*, 44:800-9, 1997.
- [4] H. Zhou, A. van Oosterom, "Computation of the potential distribution in a four-layer anisotropic concentric spherical volume conductor," *IEEE Trans. Biomed. Eng.*, 39:154-158, 1992.